Article citation info:
CHUDZIK A, WARDA B. Fatigue life prediction of a radial cylindrical roller bearing subjected to a combined load using FEM. Eksploatacja i Niezawodnosc – Maintenance and Reliability 2020; 22 (2): 212–220, http://dx.doi.org/10.17531/ein.2020.2.4.

Agnieszka CHUDZIK
Bogdan WARDA

FATIGUE LIFE PREDICTION OF A RADIAL CYLINDRICAL ROLLER BEARING SUBJECTED TO A COMBINED LOAD USING FEM

PROGNOZOWANIE TRWAŁOŚCI ZMĘCZENIOWEJ PROMIENIOWEGO ŁOŻYSKA WALCOWEGO PODDANEGO ZŁOŻONEMU OBCIĄŻENIU Z WYKORZYSTANIEM MES

The article presents the results of studies on the impact of a combined load of a radial cylindrical roller bearing for its predicted fatigue life. The distributions of maximum equivalent subsurface stresses and their depths, necessary during calculations of fatigue life, were determined using the finite element method, using the basic package of the ANSYS program. The calculations took into account the geometrical parameters of the bearing, including radial clearance and the shape of the rolling elements generators. The calculation results showed that the axial load of the radial cylindrical roller bearing and the tilt of the rollers associated with its operation reduces fatigue life. The obtained results were compared with the results of calculations according to the SKF catalogue method, obtaining satisfactory compliance.

***Keywords**: rolling bearing; stress distribution; fatigue life; finite element method; combined load.*

W artykule zaprezentowano wyniki badań wpływu złożonego obciążenia promieniowego łożyska walcowego na jego prognozowaną trwałość zmęczeniową. Rozkłady maksymalnych zastępczych naprężeń podpowierzchniowych oraz głębokości ich występowania, niezbędne podczas obliczeń trwałości zmęczeniowej, określono za pomocą metody elementów skończonych, z wykorzystaniem pakietu podstawowego programu ANSYS. W obliczeniach uwzględniono geometryczne parametry łożyska, w tym luz promieniowy i kształt tworzących elementów tocznych. Wyniki obliczeń wykazały, że obciążenie osiowe promieniowego łożyska walcowego i przechylenie wałeczków towarzyszące jego działaniu powoduje zmniejszenie trwałości zmęczeniowej. Otrzymane wyniki porównano z wynikami obliczeń według katalogowej metody firmy SKF, otrzymując zadowalającą zgodność.

***Słowa kluczowe:** łożysko walcowe, rozkład naprężeń, trwałość zmęczeniowa, metoda elementów skończonych, złożone obciążenie.*

Nomenclature

A	material constant
B	bearing width
C	dynamic load rating
D	bearing outside diameter
D_r	roller diameter
E	Young's modulus
F_r	radial load of the bearing
F_a	axial load of the bearing
$F_{ap\ max}$	permissible axial load
L_{10}	fatigue life
L_r	roller length
Q	resultant normal force in the roller-main race contact
Q_a	axial force per roller
Q_f	resultant normal force in the roller end flange contact
Q_r	radial force per roller
Z	depth of occurrence of maximal von Mises stresses along the x axis
Z_r	number of rollers in the bearing
c	exponent in the equation determining the survival probability
d	bearing bore diameter
d_{bi}	diameter of the inner ring raceway
d_{bo}	diameter of the outer ring raceway
e	Weibull slope
g	radial clearance in the bearing
h	exponent in the equation determining the survival probability
i	inner raceway (index)
j	number of roller
l	length of the roller-main race contact area
o	outer raceway (index)
r_b	radius of the main race
r_c	roller chamfer dimension
u	number of load cycles per one revolution
η	roller tilt angle
θ	roller skew angle
σ	maximal von Mises stress occurring along the x axis
ϕ	survival probability of the bearing element
ψ	angle measured along the bearing circumference
ψ_j	angle between rollers
ψ_{lim}	angle of the loaded zone

1. Introduction

In many cases, there is a need to precisely determine the fatigue life of bearing arrangements. Forecasting methods were presented in the catalogue of rolling bearings but they are not taking into account many factors affecting it. One of them is misalignment of the bearing's rings. In cylindrical rolling bearings it results in tilting rollers relative to the raceway and uneven pressure distribution in the contacts of the rollers with the raceways. Similar phenomenon can be observed in cylindrical roller bearings, which next to the radial load can carry a continuous, low axial load. These bearings include design variants NJ, NUP and NU with angular ring HJ. Occurring in the contacts of the rollers with the main raceways and auxiliary raceways (flanges), normal forces Q, Q_f and friction force T_f causes bearing tilt in two respectively perpendicular planes passing through the bearing axis. Bearing tilt in plane parallel to the bearing axis (angle θ), caused by friction force in roller contacts with flanges (Fig. 1), causes rollers precipitation from the right track and as a result occurrence of slips in roller contact with main raceways. Because of small values of θ angles, influence of phenomena associated with skewing on its fatigue life can be skipped [15]. Roller tilt in the plane passing through roller axis (angle η) causes occurrence of uneven pressure distribution in roller contacts with main raceways characterised by increased load on one end of the contact area. This phenomenon significantly reduces bearing fatigue life.

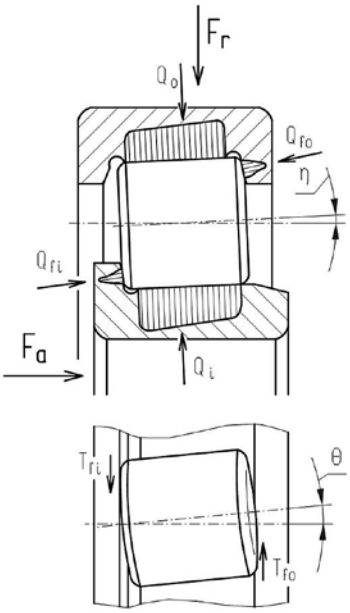

Fig. 1. Tilting η and skewing θ of the roller in the radial cylindrical roller bearing loaded with radial force F_r and axial force F_a

Until recently it was impossible to determine fatigue life of a NJ cylindrical roller bearing loaded with radial and axial force. Currently SKF company bearing catalogue [23] provides formulae allowing for approximate the fatigue life of such a loaded bearing.

According to the information in the catalogue [23] cylindrical single row bearings and cylindrical single row bearings with full number of rollers with flanges on the inner and outer ring can carry an axial load of value up to $F_a = 0.5\,F_r$. Because of mechanical limitations permissible axial load of radial cylindrical roller bearings of the dimension series 2 cannot be greater than $F_{ap\,max} = 0.0045\,D^{1,5}$. Basic nominal durability of the rolling bearing is determined from the formula:

$$L_{10} = \left(\frac{C}{P}\right)^{10/3}, \tag{1}$$

where equivalent dynamic load of the NJ series 2 radial cylindrical roller bearing equals:

$$P = F_r \qquad \text{for}: F_a / F_r \le 0.2 \tag{2}$$

$$P = 0.92\,F_r + 0.6\,F_a \qquad \text{for}: F_a / F_r > 0.2 \tag{3}$$

Precise determination of cylindrical roller bearing fatigue life subjected to a combined load is only possible using computer technology. Forecasting method of the fatigue life requires consideration of local values of subsurface stress which affects fatigue life. It is necessary to determine the radial and axial load distribution on bearing individual elements beforehand. The most convenient way to complete this task is to use finite elements method. Properly built FEM solid model, replicating internal geometry of a bearing, including correction of roller generators but also taking into account bearing clearances and mutual tilting of mating elements of the bearing caused by complex loading and misalignment of the rings, would give one the most accurate information about both load distributions as well as pressure distributions in the contacts and corresponding subsurface stress distributions.

FEM calculations require a lot of computing power and are time consuming. This is the reason why FEM models were mostly used with ball bearings [11, 22]. In studies on determining load distribution in roller bearings, the authors usually used two-dimensional FEM models [6, 16, 19, 32], and thus were unable to account for the axial force acting on the bearing, or used three-dimensional models [10, 17, 18], but they did not deal with bearings subjected to complex loading, which greatly simplified the calculation model. In many cases, to simplify the three-dimensional bearing model, rollers or balls were replaced with elements defined by the model creator, so-called super elements. Super elements were used in the studies written by Golbach [8], Kania [12] and Claesson [5]. The last researcher developed simplified FEM models for tapered roller bearings and cylindrical roller bearings, including radial cylindrical roller bearings capable of carrying a complex load. Author [5] stressed that the use of full models of solid bearings in the finite element method is unprofitable from the point of view of the cost of calculations.

Researchers often used numerical methods other than the finite element method to find load distribution on rolling bearing components. Zhenhuan et al.[33] in their work they determined load distribution on high speed cylindrical roller bearings using the quasi-dynamic method. Cheng et al., did similarly, analyzing the impact of axial load on fatigue life of a radial cylindrical roller bearing [3]. In their work, they used the methods used in the models described by Brandlein and Fernlund [2, 7]. The authors examined the general conditions of contact of rollers with bearing raceways by introducing the concept of three bearing load zones. In the first of them, the rollers are in contact with the raceways along the entire roller generator length, in the second one on the roller generator part, and in the third one they are not in contact with the raceways, and thus, they do not carry load. However, the researchers did not present the distribution of axial forces on the rollers, focusing on determining the impact of uneven pressure distribution in the contacts of the rollers with the main raceways on bearing fatigue life. Another study that the authors did not use the finite element method is an article by Tong et al. dealing, among others, about the impact of bearing rings misalignment on its fatigue life [26]. The authors built a quasi-static cylindrical bearing model with four degrees of freedom, and numerically solved the system of bearing equilibrium equations, and then, by solving the Boussinesq problem for elastic half-space, determined the pressure distributions at the contacts enabling the calculation of the predicted fatigue life.

The authors of this article have also used a method that does not use finite elements in their previous works. The radial and axial load distributions were determined by solving the system of equations of rings and rollers by numerical way. Resultant normal forces Q oc-

curring in the contacts of the rollers with the main raceways and the location of their application points were determined on the basis of the Palmgren formula [20, 21], while to calculate the resultant forces Q_f in the contacts of the roller faces with flanges, a calculation model was used, in which the contact area was divided into a number of layers of a defined, small width, and the pressure distribution under each of the layers was determined as for a rigid punch with an infinite length pressed under given angle in elastic half-space [27, 28]. Knowledge of load distributions enabled the authors to find subsurface stress distributions in the contacts and to calculate the predicted bearing fatigue life. The authors used this method to analyse the impact on fatigue life of radial cylindrical roller bearing correction roller generators [28], misalignment of bearing rings [29] and radial clearance in the bearing [4].

In all cited studies, the authors of this article used the finite element method to determine the distribution of subsurface stress, regardless of the solution of the Boussinesq problem for elastic half-space. For this purpose, three-dimensional models of the bearing fragment were built, which included a rolling element (roller) and a segment of one of the bearing rings [28, 29] or parts of both rings [4]. Consideration of the FEM model for a bearing fragment instead of the full solid model is commonly used by numerous researchers in a situation where the main purpose of the analysis is to study phenomena occurring in a single contact of rolling elements [1, 9, 24, 25, 30, 31]. The author of the work [13], who studied the influence of fitting and initial deformation on the resistance to motion in an angular-contact ball bearing, did a similar way. The author described in the work the analytical model of the angular contact ball bearing, but due to its complexity he used the finite element method to solve the problem, analysing a fragment of the bearing.

This paper discusses the impact of a combined load on the fatigue life of a radial cylindrical roller bearing. The task was carried out using the method described in works [27, 28], but only the finite element method was used to determine the subsurface stress distribution determining fatigue life.

2. Method for determining fatigue life of a radial cylindrical roller bearing

Predicted fatigue life of radial cylindrical roller bearing subjected to a combined load was calculated using the method described in the papers [27, 28], and also used in the works [4, 29]. This method is based on the basic assumptions of the commonly used fatigue life forecasting model developed by Lundberg and Palmgren [20, 21].

Determination of fatigue life L_{10} of a complete bearing requires an independent calculation of the durability of the inner L_{10i} and outer L_{10o} ring:

$$L_{10} = \left(L_{10i}^{-e} + L_{10o}^{-e} \right)^{-1/e} . \tag{4}$$

Durability of the inner ring, which is usually a rotating ring relative to the load, is determined from the relationship determining the inverse logarithm of the probability of durability φ_i:

$$ln\frac{1}{\varphi_i} = A \cdot u_i^e \; L_{10i}^e \; 2\pi \left[\frac{1}{2\pi} \int_0^{2\pi} \left(\int_0^l r_{bix} \; \sigma_{ix\psi}^c \; Z_{ix\psi}^{1-h} \; dx \right)^{1/e} d\psi \right]^e . \tag{5}$$

The durability of the outer ring, usually stationary, is calculated from a similar equation:

$$ln\frac{1}{\varphi_o} = A \cdot u_o^e \; L_{10o}^e \int_0^{2\pi} \int_0^l r_{box} \; \sigma_{ox\psi}^c \; Z_{ox\psi}^{1-h} \; dx \, d\psi , \tag{6}$$

where $\varphi_i = \varphi_o = 0.9$.

In the above formulae L_{10} is the number of revolutions of the bearing, u the number of load cycles per revolution, $\sigma_{x\psi}$ is maximum subsurface stress determined in accordance with the Huber-Mises-Hencke hypothesis (or in other words, von Mises stress), and $Z_{x\psi}$ is depth at which these stresses occur (Fig. 2). For the bearing to be considered, the material constant $A = 4.5 \cdot 10^{-40}$. The values of the exponents found in both equations are: $c = 31/3$, $h = 7/3$, $e = 9/8$. The method of deriving the formulae (5, 6) is presented in study [27].

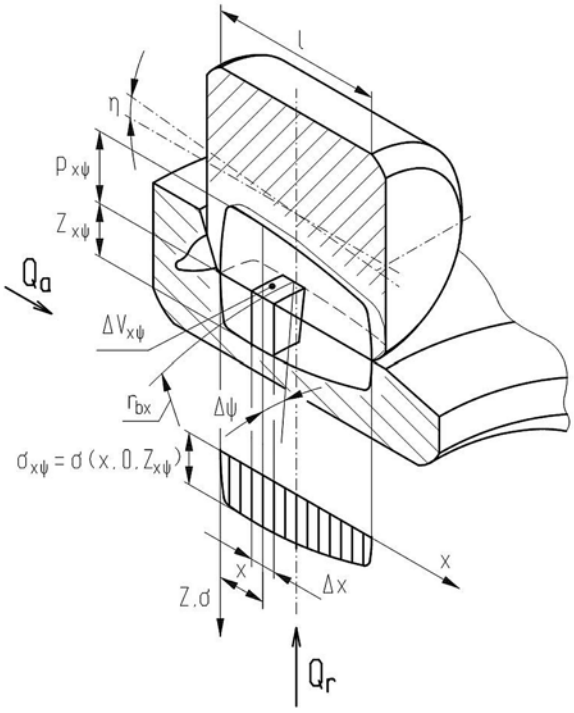

Fig. 2. Distributions of pressure and subsurface stresses deciding on fatigue life of radial cylindrical roller bearing subjected to combined load

Equations (5) and (6) were solved by numerical integration using a computer program ROLL2 [27]. Earlier, the distribution of maximum substitute subsurface stresses σ were found using the finite element method in the contact area between the rollers and raceways and the depth of their occurrence Z. To determine them, it was necessary to know the values of forces acting in contacts of subsequent rollers with the main raceways of the bearing as well as the tilt angles of the rollers $\eta = \eta_i = \eta_o$. They were determined using a computer program ROLL1, built based on the method described in the works [27, 28].

3. Determination of subsurface stresses and their depth of occurrence using FEM

Numerical calculations were done using the ANSYS program. Calculations for a complete bearing model requires a computer with very high computing power. Therefore, the calculations were carried out for the model comprising a single roller and a fragment of the outer or inner race. For this purpose, a numerical 3D solid model mapping the internal geometry of the bearing was built, which includes modified logarithmic correction of roller generators. The method of determining the value of forces acting on the rollers and the angles of inclination of the rollers relative to the raceways necessary to perform the numerical calculations are described in chapter 5.

Symmetry conditions of the tested bearing enabled the authors of the work to model half the roller and the corresponding part of the raceway of the inner or outer ring. Part of the raceway under consid-

eration resulted from the dimensions of the bearing and the number of rollers in the tested bearing. Key point in the researching rolling bearings is the roller contact zone with the raceway. Strongly non-linear phenomena occur there, which is why it is very important to create contact pairs and proper setting of contact parameters. FEM systems do not allow to geometrically model curvilinear objects. The roller cross section, i.e. the circle, is a broken line, this is due to the fact that the examined 3D model is divided into finite elements. For this reason, the results of calculations obtained by numerical method strictly depend on the number of elements resulting from the division of the examined object into finite elements which in the case of contact phenomena is particularly important. For this reason, the division into elements in the area of anticipated contact has been increased and an uneven division of contact elements in this area has been used. The contact model was used for calculations in the contact zone: TARGE surface type to CONTA surface type of the contact. While analysing the character of the roller contact with the bearing raceways, calculations assumed the roller surface as the contact surface. The surface of the raceway was assumed as the target surface. The contact surface was modelled using contact elements Conta175 and the target surface was modelled using elements Targe170. For selected roller volumes in the contact zone, the edge is divided into equal 0.05 mm length parts. The edge of selected raceway volumes was divided into equal parts with a length of 0.1 mm. Because the length of the assumed element in the contact zone (0.05 mm) is less than half the width of the contact surface, which ranges between 0.1 mm up to 0.2 mm, the division assumed was considered appropriate to ensure reliable results.

In the numerical model of the non-contact part of the bearing, 8-node solid elements of the type SOLID185 were used. The numerical model under study was divided into 752540 solid finite elements. The distance between the raceway nodes and the roller are adjustable using angle which eliminated any possible shape errors. The calculations included symmetry conditions and degrees of freedom resulting from real working conditions. ALLDOF type displacement has been taken from the outer surfaces of the outer and inner race. The lateral surfaces of the outer and inner race are deprived of the possibility of displacement in the direction of the z axis. Conditions of symmetry of the model relative to the plane y-z were imposed. The coefficient of contact stiffness was assumed for calculations FKN=1.5 calculated according to the method described in paper [14]. The Augmented Lagrange method was used. Other values of the coefficients characterising the contact were left as default.

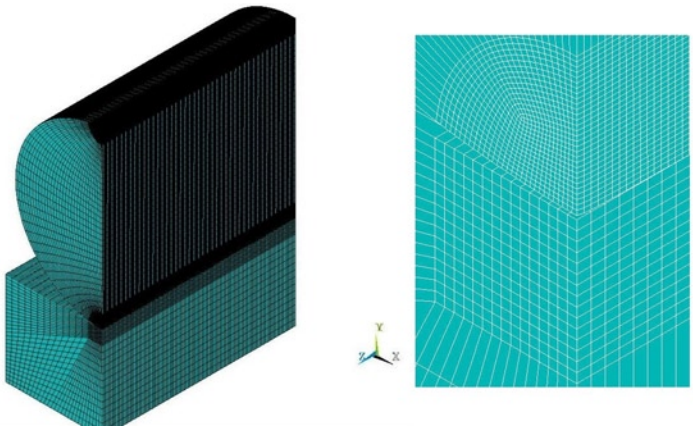

Fig. 3. 3D numerical model of the roller-raceway contact

4. Researched object

The researched object was a radial cylindrical roller bearing NJ 213 ECP that can carry an axial load [23]. The parameters of the analysed bearing are shown in Table 1.

Table 1. Parameters of the NJ 213 ECP cylindrical roller bearing [23]

Bearing bore diameter	d = 65 mm
Bearing outside diameter	D = 120 mm
Bearing width	B = 23 mm
Diameter of the outer ring raceway	d_{bo} = 108.5 mm
Diameter of the inner ring raceway	d_{bi} = 78.5 mm
Roller diameter	D_r = 15 mm
Roller length	L_r = 15 mm
Roller chamfer dimension	r_c = 0.5 mm
Number of rollers in the bearing	Z_r = 16
Dynamic load rating	C = 122000 N
Permissible axial load	$F_{ap\ max} \leq$ 5915 N

It was assumed that the profile of roller generators describes the curve corresponding to the modified logarithmic correction with the same parameters as correction of bearing rollers being the subject of analyses in the works [4, 29] (Fig. 4).

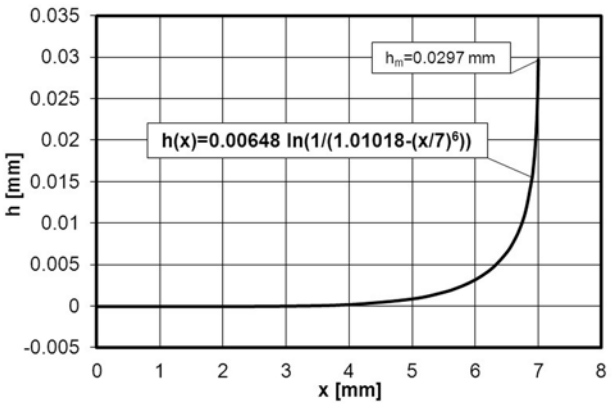

Fig. 4. Roller generator profile with a modified logarithmic correction [4, 29]

5. Radial and axial load distributions

Calculations of fatigue life of a radial cylindrical roller bearing were carried out for two values of radial load F_r, forming 10% and 20% of the dynamic bearing capacity of bearing C. First value, $F_r = 0.1\ C$, is similar to the radial load to which radial cylindrical roller bearings of the type NJ and NUP, used in the axle boxes of a typical passenger and freight bogie, are subjected. Second one, $F_r = 0.2\ C$, corresponds to the average radial load for general purpose cylindrical roller bearings, such as analysed NJ 213 ECP bearing. The axial force used in the calculations was of equal value in both cases, not exceeding the permissible value of axial load $F_{ap\ max}$. In the first case it was $F_a = 0.4\ F_r$, in second $F_a = 0.2\ F_r$. For comparison, calculations were also made only for radial loading, i.e. the case $F_a = 0$. It was assumed that the axes of both bearing rings remain parallel. The methodology used allows one to set any clearance value, both positive and negative. The value of radial clearance in the bearing $g = 0$ was taken for calculations.

Table 2. Radial and axial load distributions on NJ 213 ECP bearing rollers

Radial load		F_r = 0.1 C = 12200 N			F_r = 0.2 C = 24400 N		
Axial load		F_a = 0.4 F_r = 4880 N			F_a = 0.2 F_r = 4880 N		
ψ_{lim} [°]		147.78			116.8		
Roller No.	ψ_j [°]	Q_{rj} [N]	Q_{aj} [N]	η_j [']	Q_{rj} [N]	Q_{aj} [N]	η_j [']
1	0	3125	591	1.587	6224	625	1.566
2	22.5	2865	587	1.589	5701	620	1.566
3	45	2138	572	1.599	4241	603	1.569
4	67.5	1148	528	1.647	2159	569	1.588
5	90	456	327	1.986	453	324	1.973
6	112.5	131	117	2.411	12	12	2.704
7	135	14	14	2.711	0	0	0
8	157.5	0	0	0	0	0	0
9	180	0	0	0	0	0	0

Radial load		F_r = 0.1 C = 12200 N			F_r = 0.2 C = 24400 N		
Axial load		F_a = 0			F_a = 0		
ψ_{lim} [°]		90			90		
Roller No.	ψ_j [°]	Q_{rj} [N]	Q_{aj} [N]	η_j [']	Q_{rj} [N]	Q_{aj} [N]	η_j [']
1	0	3114	0	0	6228	0	0
2	22.5	2852	0	0	5704	0	0
3	45	2119	0	0	4238	0	0
4	67.5	1071	0	0	2142	0	0
5	90	0	0	0	0	0	0
6	112.5	0	0	0	0	0	0
7	135	0	0	0	0	0	0
8	157.5	0	0	0	0	0	0
9	180	0	0	0	0	0	0

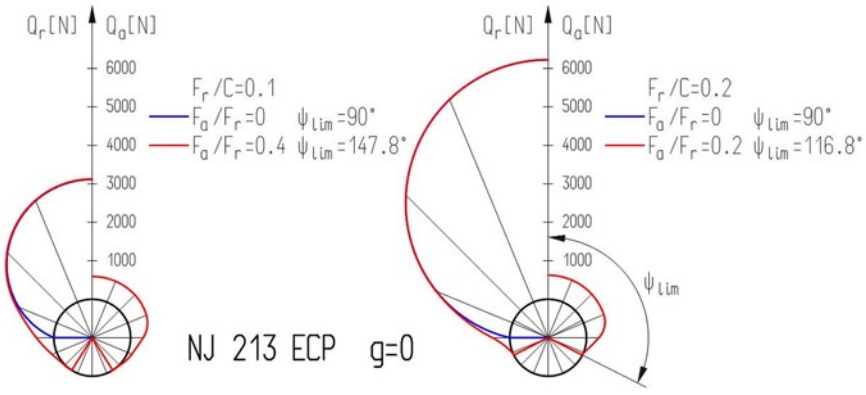

Fig. 5. The distributions of radial and axial load on the rollers of NJ 213 ECP bearing

The results of calculations of load distributions, obtained using the program ROLL1 [27], is shown in Table 2 and illustrated in figures 5 and 6.

As can be seen from the table and what can be seen in Figure 7, along with the increase in axial load, due to the rollers tilting (Fig. 8), the size of the loaded zone of bearing rollers increases. Its value is determined by the angle ψ_{lim}. It can also be seen that only rollers loaded with radial force can simultaneously carry axial load.

6. Distribution of maximum subsurface stress and their depth of occurrence

To calculate the predicted bearing fatigue life, knowledge of the maximum subsurface stress distributions along the roller-raceway contact line σ_{xj} and the depth distributions of these maximum stresses Z_{xj}, where j is the number of the next roller, is required. Distributions of maximum subsurface stresses were found using FEM method. For calculations, it was assumed that the rolling elements are made of elastic-ideally plastic material. The material properties were determined by Young's modulus E = 208 GPa, Poisson's ratio v = 0.3 and the tensile yield strength σ_o = 1950 MPa.

The ANSYS program allows one to illustrate stress distributions, values and locations of maximum and minimum stress in the form of maps. Sample stress maps for rollers number 1, 3, 5, 6 and loads F_r = 0.2 C, F_a = 0.2 F_r are shown in figures 7, 8, 9 and 10. The program also allows one to get charts showing the maximum stress distributions along the roller contact line with the raceway, but it is not possible to directly obtain the distribution of the depth of maximum stresses. Basic ANSYS package only allows finding subsurface stress distribution in any plane

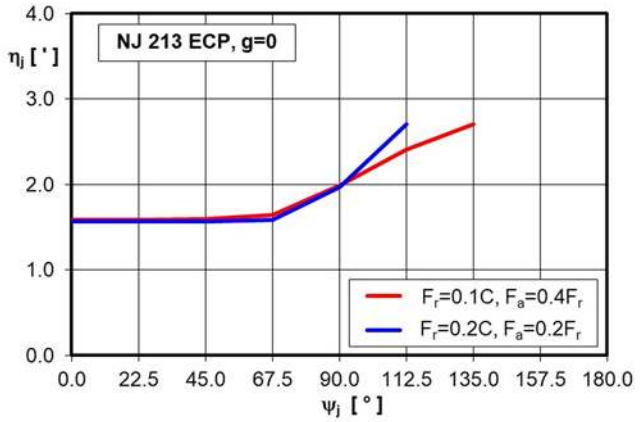

Fig. 6. Roller tilt angle η_j as a function of the angle ψ_j that determines the position of the roller in the bearing

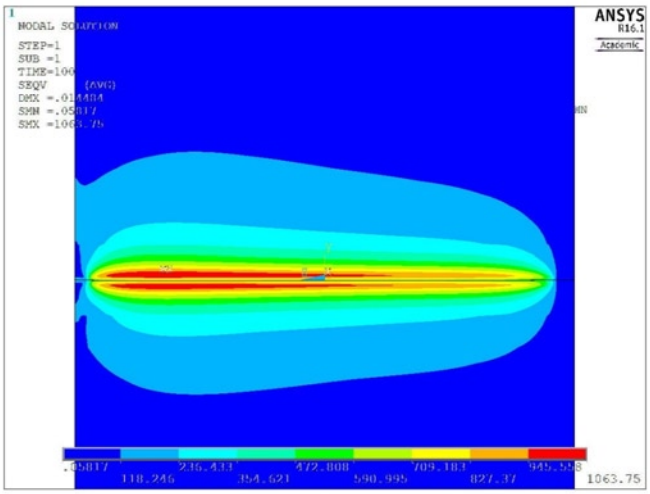

Fig. 7. Distributions of von Mises stresses below the roller-inner ring raceway contact surface; roller No.1, F_r = 0,2 C, F_a = 0,2 F_r

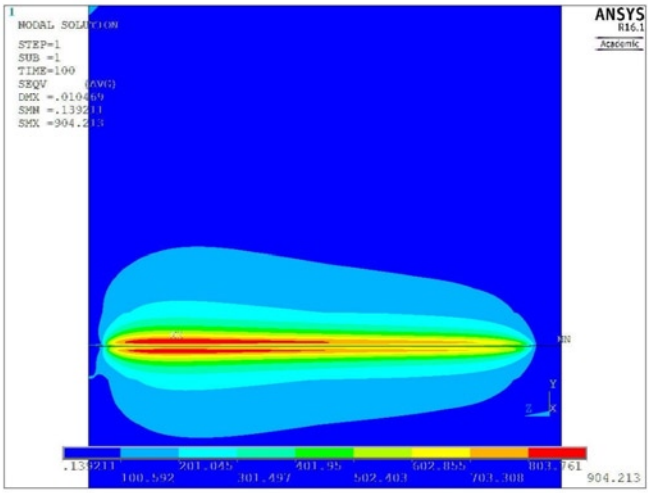

Fig. 8. Distributions of von Mises stresses below the roller-inner ring raceway contact surface; roller No.3, F_r = 0,2 C, F_a = 0,2 F_r

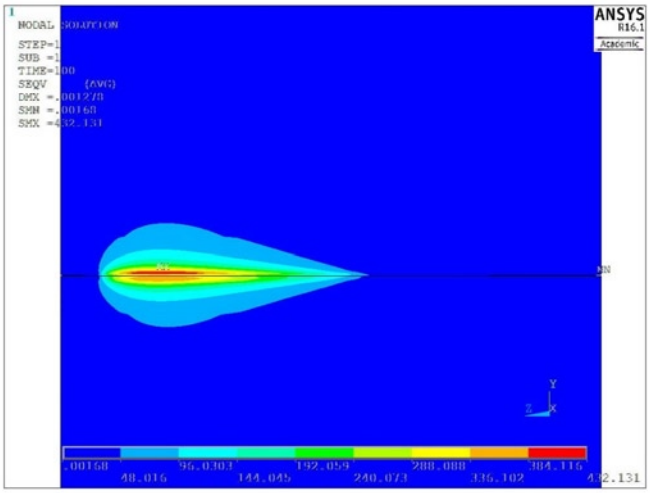

Fig. 9. Distributions of von Mises stresses below the roller-inner ring raceway contact surface; roller No.5, F_r = 0,2 C, F_a = 0,2 F_r

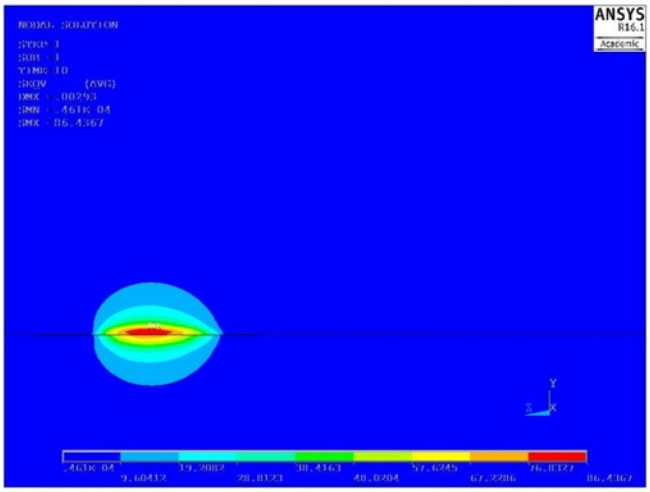

Fig. 10. Distributions of von Mises stresses below the roller-inner ring raceway contact surface; roller No.6, F_r = 0,2 C, F_a = 0,2 F_r

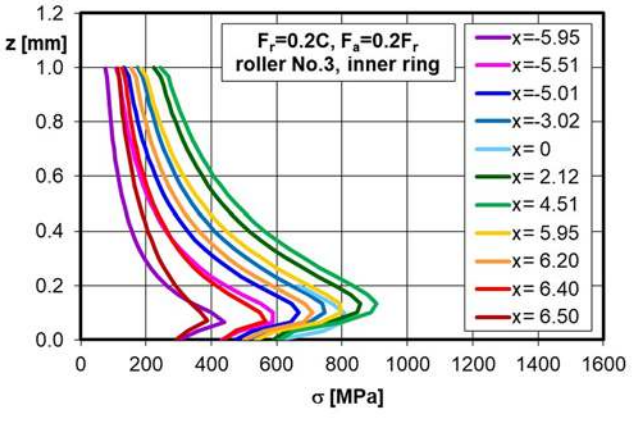

Fig. 11. Distribution of von Mises stresses in in selected cross-sections of the roller-inner ring raceway contact

specified by the user. By examining changes in subsurface stresses in selected sections, the distribution of the depth of occurrence of maximum subsurface stresses along the contact line of rolling elements can be determined. The same procedure was used to search for the distribution of the occurrence of maximum subsurface stress at study [4]. An example of a graph that allows finding the depth of occurrence of maximum subsurface stress is shown in Figure 11.

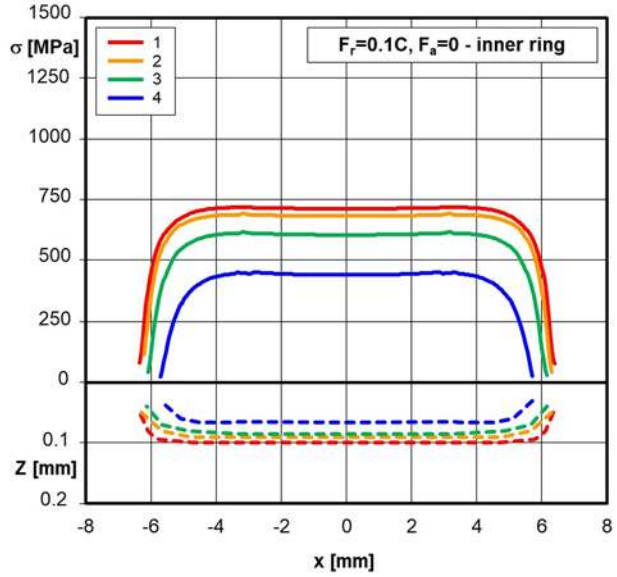

Fig. 12. Distributions of maximal von Mises stresses σ and the depth of their occurrence Z in contacts of subsequent rollers with the inner ring raceway; F_r = 0,1 C, F_a = 0

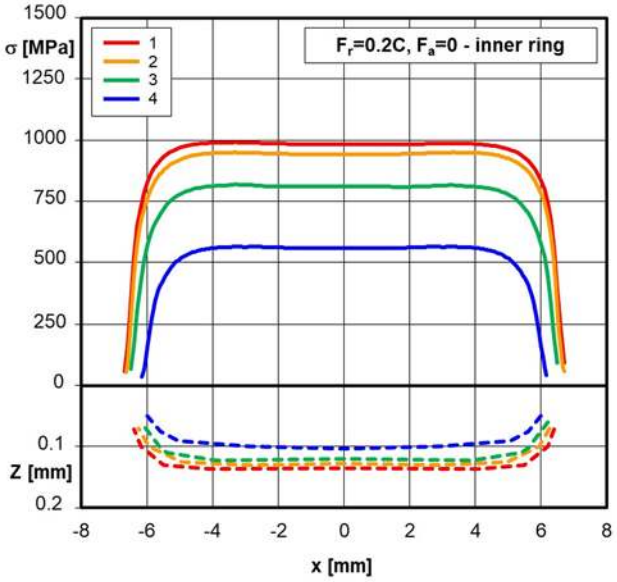

Fig. 13. Distributions of maximal von Mises stresses σ and the depth of their occurrence Z in contacts of subsequent rollers with the inner ring raceway; F_r = 0,2 C, F_a = 0

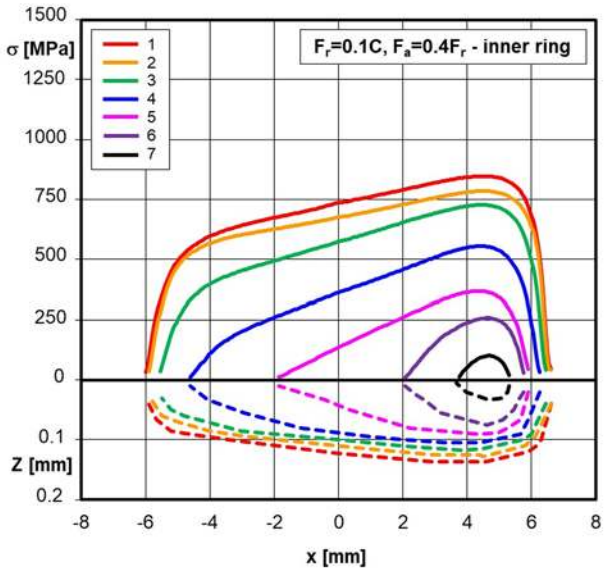

Fig. 14. Distributions of maximal von Mises stresses σ and the depth of their occurrence Z in contacts of subsequent rollers with the inner ring raceway; F_r = 0,1 C, F_a = 0,4 F_r

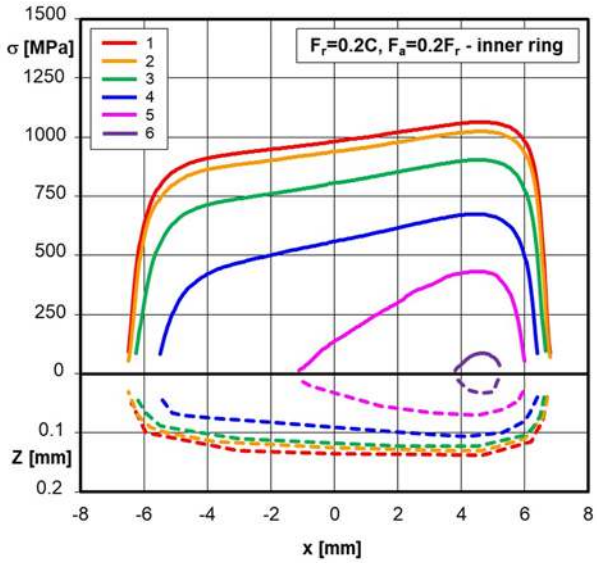

Fig. 15. Distributions of maximal von Mises stresses σ and the depth of their occurrence Z in contacts of subsequent rollers with the inner ring raceway; F_r = 0,2 C, F_a = 0,4 F_r

In figures 12, 13, 14 and 15 distributions of the maximum subsurface stress σ and the depth of their occurrence Z in roller contacts with the inner ring race obtained by FEM are presented. The numbers next to the coloured lines shown in the legend correspond to the numbers of consecutive load-bearing rollers (compare: Table 2).

Two first charts present distributions for cases where the bearing is only loaded with radial force: $F_r = 0.1\ C$ (Fig. 12) and $F_r = 0.2\ C$ (Fig. 13). The stress distribution σ and the depth of their occurrence Z are characterised by symmetry. Thanks to the logarithmic correction of the forming rollers, no stress accumulation occurs in the contacts but the length of the contact area of even the most loaded roller is less than the length of the forming roller l (Fig. 2) and decreases as the radial force on the roller decreases. As one can see, the logarithmic correction protects against pressure accumulation at the edges of the rollers, but prevents the roller working surface from being fully used.

The next two graphs illustrate stress distribution σ and their depth of occurrence Z for the bearing subjected, next to the radial load $F_r = 0.1\ C$ i $F_r = 0.2\ C$, to the axial load equal respectively: $F_a = 0.4\ F_r$ (Fig. 14) and $F_a = 0.2\ F_r$ (Fig. 15). Roller tilt relative to raceways due to axial load results in uneven stress distribution in the contacts, characterized by an increase in stress at one end of the contact field. In the load-bearing rollers area, the size of which is determined by the angle ψ_{lim}, two areas can be distinguished. In the first area, the rollers are in contact with the raceways virtually along the entire generator length, although in this case as well as for $F_a = 0$, the contact field length is always smaller than the length l. In the second area, the contact only exists on the roller generator part, in extreme cases, for rollers lying near the end of the loaded zone, the contact area is located at the very edge of the roller working surface (roller number 7 for $F_r = 0.1\ C$ and $F_a = 0.4\ F_r$, roller number 6 for $F_r = 0.2\ C$ and $F_a = 0.4\ F_r$, Fig. 10,

11). The authors of the study [3] noted the occurrence of similar bearing loaded zones.

7. Fatigue life of a bearing subjected to combined load

Distributions of maximum subsurface stress and depth of their occurrence at the contacts of rollers with inner and outer ring raceways obtained using FEM allowed for calculation of the predicted fatigue life of the NJ 213 ECP bearing.

In Table 3 the results of calculations of the predicted fatigue life of the tested bearing for the considered load cases were summarised. The durability of a bearing loaded only with radial force was compared with the durability of a bearing subjected to a combined load. In addition, the table presents the results of calculations of fatigue life according to formulae (1), (2) and (3) in accordance with the SKF catalogue method [23].

The two methods used to calculate the predicted fatigue life, numerical using stress information obtained using FEM and the catalogue method, give comparable results. Numerical method at lower radial loads (F_r = 0.1 C) gives results of the predicted durability slightly overstated compared to the catalogue method, and at higher loads (F_r = 0.2 C) understated. The axial load of the radial cylindrical roller bearing and the associated tilting of the rollers reduces fatigue life. The numerical method allows one to capture a decrease in durability even with an axial load that is a small part of the radial load (F_r = 0.2 C, F_a = 0.2 F_r, decrease in durability by 11% compared to durability for F_a = 0). In such cases, the catalogue method ignores the impact of axial load on fatigue life. The impact of axial load is taken into account by the catalogue method only after exceeding the threshold value, i.e. for F_a / F_r > 0.2. Then the predicted fatigue life of the bearing decreases abruptly. For the case F_r = 0,1 C and F_a = 0,4 F_r bearing life determined according to the catalogue method is reduced by 39% compared to the life of F_a = 0. The predicted fatigue life determined by the numerical method decreases to a lesser extent. For the present case, the decrease in durability compared to durability for F_a = 0 is 17%.

Numerical method using previously determined distributions of maximum subsurface stress and their depth in contact of rolling elements, enables more precise forecasting of fatigue life of a radial cylindrical roller bearing subjected to combined loading than allowed by catalogue methods. In addition, it allows one to take into account other factors affecting bearing durability, such as correction of forming rolling elements, or bearing clearance. The practical application of the proposed method reduces the need for time-consuming calculations of subsurface stresses using FEM. However, this time can be greatly reduced by using the Boussinesq solution for elastic half-space to determine the stress [4, 28, 29], which gives results comparable to FEM.

8. Summary

The article is dedicated to forecasting fatigue life of a radial cylindrical roller bearing type NJ loaded with radial and axial force. For forecasting, a numerical method using the maximum subsurface stress distributions and their depth in contact of rolling elements determined using the finite element method was used. Distribution of radial and axial forces for the analysed load cases, as well as the distribution of maximum stresses and their location along the contact line with the raceways of subsequent load-bearing rollers are presented. It has been demonstrated that the axial load of a radial cylindrical roller bearing and the associated tilting of rollers reduces fatigue life. The results of calculations of fatigue life obtained using the proposed method were compared with the results obtained according to the catalogue method, obtaining sufficient compliance.

The numerical methodology used in this work allows to include in the calculations of durability the impact of local changes in subsurface stresses in the contacts of mating elements, thanks to which it is possible to take into account many factors usually overlooked in engineering methods, described in catalogues of rolling bearings.

The most important factor is the combined bearing load, which impact on fatigue life is included in the catalogue methods in an approximate way in the form of dependence on the equivalent bearing load. The numerical method allows to accurately determine the predicted fatigue life of a bearing subjected to combined loading for any load combination.

Radial clearance is another important factor affecting the life of a cylindrical roller bearing. Radial clearance equal to zero was assumed in the calculations whose results were presented in the article, but it was possible to set a different value of the clearance, both positive and negative.

The last factor that affects the fatigue life of the bearing and which was included in the research is the correction of roller generators. Defining a generator profile is required when performing numerical calculations of pressure distributions. This makes it difficult to calculate the life of bearings with unknown profile geometry, however it allows one to optimise the correction parameters that create for the greatest fatigue life of the bearing operating under certain conditions.

References

1. Benchea M, Iovan-Dragomir A, Cretu S. Misalignment effects in cylindrical roller bearings. Applied Mechanics & Materials 2014; 658-659: 277-282, https://doi.org/10.4028/www.scientific.net/AMM.658.277.
2. Brandlein J. The fatigue life of axially loaded cylindrical roller bearings. FAG, Ball and Roller Bearing Engineering 1972; 1: 7-11.
3. Cheng W W, Shih S, Grace J, et al. Axial load effect on contact fatigue life of cylindrical roller bearings. ASME Journal of Tribology 2004; 126: 242-247, https://doi.org/10.1115/1.1614823.
4. Chudzik A, Warda B. Effect of radial internal clearance on the fatigue life of the radial cylindrical roller bearing. Eksploatacja i Niezawodnosc - Maintenance and Reliability 2019; 21 (2): 211-219, https://doi.org/10.17531/ein.2019.2.4.
5. Claesson E. Modelling of roller bearings in ABAQUS. Chalmers, Applied Mechanics, Master's Thesis, Göteborg, Sweden, 2014: 1-38.
6. Demirhan N, Kanber B. Stress and displacement distribution on cylindrical roller bearing rings using FEM. Mechanics Based Design of Structures and Machines 2008; 36: 86-102, https://doi.org/10.1080/15397730701842537.
7. Fernlund I, Synek V. Influence of axial loads on the life of cylindrical roller bearings. SKF, The Ball Bearing Journal 1967; 151: 21-26.
8. Golbach H. Integrated non-linear FE module for rolling bearing analysis. INA reprint "Proceedings of NAFEMS WORLD CONGRESS '99 on Effective Engineering Analysis", Vol. 2, Newport, Rhode Island, USA, 25-28 April 1999: 1-12.
9. Göncz P, Ulbin M, Glodež S. Computational assessment of the allowable static contact loading of a roller-slewing bearing's case-hardened raceway. International Journal of Mechanical Sciences 2015; 94 95: 174-184, https://doi.org/10.1016/j.ijmecsci.2015.03.006.
10. Guo Y, Parker R G. Stiffness matrix calculation of rolling element bearings using a finite element/contact mechanics model. Mechanism and Machine Theory 2012; 51: 32-45, https://doi.org/10.1016/j.mechmachtheory.2011.12.006.
11. Kang Y, Shen P, Huang C, Shyr S, Chang Y. A modification of the Jones-Harris method for deep-groove ball bearings. Tribology International

2006; 39: 1413-1420, https://doi.org/10.1016/j.triboint.2005.12.005.
12. Kania L. Modelling of rollers in calculation of slewing bearing with the use finite elements. Mechanism and Machine Theory 2006; 41: 1359-1376, https://doi.org/10.1016/j.mechmachtheory.2005.12.007.
13. Kosmol J. Extended model of angular bearing - influence of fitting and pre-deformation. Eksploatacja i Niezawodnosc - Maintenance and Reliability 2019; 21 (3): 493-500, https://doi.org/10.17531/ein.2019.3.16.
14. Harris TA, Kotzalas MN. Rolling Bearing Analysis, Fifth Edition -2 Volume Set. CRC Press; 2007, https://doi.org/10.1201/9781482275148.
15. Krzemiński-Freda H, Warda B. The effect of roller end-flange contact shape upon frictional losses and axial load of the radial cylindrical roller bearing. Proc. of the 15th Leeds-Lyon Symp. on Tribology, 6th-9th September 1988: 287-295, https://doi.org/10.1016/S0167-8922(08)70205-0.
16. Laniado-Jácome E: Numerical model to study of contact force in a cylindrical roller bearing with technical mechanical event simulation. Journal of Mechanical Engineering and Automation 2011; 1 (1): 1-7, https://doi.org/10.5923/j.jmea.20110101.01.
17. Lee J, Pan J. Closed-form analytical solutions for calculation of loads and contact pressures for roller and ball bearings. Tribology International 2016; 103: 187-196, https://doi.org/10.1016/j.triboint.2016.06.042.
18. Li S. A mathematical model and numeric method for contact analysis of rolling bearings. Mechanism and Machine Theory 2018; 119: 61-73, https://doi.org/10.1016/j.mechmachtheory.2017.08.020.
19. Liu J, Shi Z, Shao Y. An investigation of a detection method for a subsurface crack in the outer race of a cylindrical roller bearing. Eksploatacja i Niezawodnosc - Maintenance and Reliability 2017; 19 (2): 220-228, https://doi.org/10.17531/ein.2017.2.8.
20. Lundberg G, Palmgren A. Dynamic capacity of rolling bearings. Acta Polytech Scand Mech Eng 1947; 1(3): 1-52.
21. Lundberg G, Palmgren A. Dynamic capacity of roller bearings. Acta Polytech Scand Mech Eng 1952; 2(4): 96-127.
22. Łazarz B., Peruń G., Bucki S.: Application of the finite-element method for determining the stiffness of rolling bearings. Transport Problems 2008; 3 (3): 33-40.
23. Łożyska toczne SKF. PUB BU/P1 10000 PL, 2014.
24. Poplawski J V, Peters S , Zaretsky E V. Effect of roller profile on cylindrical roller bearing life prediction - Part II Comparison of roller profiles. Tribology Transactions 2001; 44 (3): 417-427, https://doi.org/10.1080/10402000108982476.
25. Shah Maulik J, Darji P H. Fatigue life improvement through reduction of edge pressure in cylindrical roller bearing using FE analysis. International Journal For Technological Research in Engineering 2014; 1 (10): 1069-1074.
26. Tong V C, Kwon S W, Hong S W. Fatigue life of cylindrical roller bearings. Proc IMechE Part J: J Engineering Tribology 2016; 231: 623-636, https://doi.org/10.1177/1350650116668767.
27. Warda B. Wykorzystanie istniejących teorii zmęczenia powierzchniowego do prognozowania trwałości złożonych węzłów tocznych. Zeszyty Naukowe PŁ, Łódź 2009; 1055 (386): 1-159.
28. Warda B, Chudzik A. Fatigue life prediction of the radial roller bearing with the correction of roller generators. International Journal of Mechanical Sciences 2014; 89: 299-310, https://doi.org/10.1016/j.ijmecsci.2014.09.015.
29. Warda B, Chudzik A. Effect of ring misalignment on the fatigue life of the radial cylindrical roller bearing. International Journal of Mechanical Sciences 2016; 111-112: 1-11, https://doi.org/10.1016/j.ijmecsci.2016.03.019.
30. Xia X, Zhu S, Jia C, Niu R. Study of interval of arc modification length of cylindrical roller using ANSYS. International Journal of Engineering and Science 2012; 1 (1): 8-13.
31. Xia X, Shang Y, Zhu S. Effects of misalignment in cylindrical roller bearings on contact between roller and inner ring. IOSR Journal of Engineering 2013; 3 (5): 1-8, https://doi.org/10.9790/3021-03540108.
32. Zhao H: Analysis of load distributions within solid and hollow roller bearings. ASME Journal of Tribology 1998; 120: 134-139, https://doi.org/10.1115/1.2834176.
33. Zhenhuan Y, Liqin W, Le G, Chuanwei Z. Effects of tilted misalignment on loading characteristics of cylindrical roller bearings. Mechanism and Machine Theory 2013; 69:153-167, https://doi.org/10.1016/j.mechmachtheory.2013.05.006.

Agnieszka CHUDZIK
Department of Dynamics
Lodz University of Technology
Stefanowskiego 1/15, 90-537 Lodz, Poland

Bogdan WARDA
Department of Vehicles and Fundamentals of Machine Design
Lodz University of Technology
Stefanowskiego 1/15, 90-537 Lodz, Poland

E-mails: agnieszka.chudzik@p.lodz.pl, bogdan.warda@p.lodz.pl